



## Effect of Iodide on the Corrosion Inhibitive Behaviour on Carbon Steel by an Azomethine Compound Derived from Anthracene-9(10 H)-one

K.S. SHAJU, K. JOBY THOMAS\* and VINOD P. RAPHAEL

Department of Chemistry, St. Thomas' College (University of Calicut), Thrissur, Kerala, India.

\*Corresponding author E-mail: drjobythomask@gmail.com

<http://dx.doi.org/10.13005/ojc/300255>

(Received: April 03, 2014; Accepted: May 16, 2014)

### ABSTRACT

The inhibition effect of (s)-2-(anthracene-9(10H)-ylideneamino)-5-guanidinopentanoic acid (A9Y5GPA) on carbon steel (CS) in 0.5 M sulphuric acid solution has been investigated using weight loss measurements, electrochemical impedance spectroscopy (EIS) and potentiodynamic polarization studies. The addition of KI to A9Y5GPA enhanced the inhibition efficiency due to synergistic effect. The adsorption of A9Y5GPA and A9Y5GPA+ KI on the carbon steel surface obeys Freundlich and Langmuir adsorption isotherm respectively. The result showed that compound studied was acted as a mixed type inhibitor causing blocking of active sites on the metal. Surface morphology of the carbon steel specimens was evaluated by SEM analysis.

**Key words:** Carbon Steel, Adsorption, Weight loss, Isotherm, Synergism, Impedance, Polarization.

### INTRODUCTION

An effective method employed by corrosion engineers to control the corrosion of metal is the use of certain organic inhibitors<sup>1</sup>. Organic molecules possessing azomethine linkage (C=N) act as effective potential corrosion inhibitors<sup>2-6</sup>. The presence of halide ions in solutions has been found to stabilize the adsorption of some organic cations, leading to improved inhibition efficiency<sup>7</sup>. In continuation of our work<sup>8</sup>, we report in this paper the corrosion inhibition behaviour and synergism

mechanism with I<sup>-</sup> of a azomethine compound (A9Y5GPA) derived from anthracene-9(10H)-one and (s)-2-amino-5-guanidinopentanoic acid in 0.5M H<sub>2</sub>SO<sub>4</sub> solution on CS at 303 K.

### EXPERIMENTAL

#### A9Y5GPA Solutions

The azomethine compound was synthesized and characterized through their spectral data<sup>8</sup>. The molecular structure of the compound is shown in the figure 1.

The aggressive solution of 0.5M H<sub>2</sub>SO<sub>4</sub> was prepared by the dilution of A.R grade 98% of H<sub>2</sub>SO<sub>4</sub> (Merck) with de-ionized water. A9Y5GPA solutions were prepared in the range, 0.2mM-1mM concentrations. 0.2 mM KI solution was also prepared.

### Weight Loss Measurements

Weight loss experiments were performed with CS specimens of dimension 1.5x 2x 0.1 cm (Composition: C,0.5%; Mn,0.07%; P,0.02%; S,0.015%; Si,0.02% and rest Fe). The specimens were first polished with different grades of emery papers, rinsed with ethanol and water, respectively. Then dried, weighed and immersed in 50 ml corrosive medium with and without different concentrations of A9Y5GPA and A9Y5GPA + 1ml KI solutions. Weight loss of metal specimens was noted after 24 h. The corrosion rate ( $\frac{1}{2}$ ) and the percentage of inhibition efficiency (w%) were calculated by the following equations<sup>9, 10</sup>.

$$= \frac{W}{St} \quad \dots(1)$$

$$\eta \% = \frac{W - W'}{W} \times 100 \quad \dots(2)$$

where W is the weight loss (g) of coupon, S is the total area (cm<sup>2</sup>) of specimens, t is the time of treatment (24 hrs),  $\frac{1}{2}$  and  $\frac{1}{2}$  are the corrosion rates of uninhibited and inhibited specimens respectively.

### Electrochemical Investigations

The impedance measurements and polarization curves were performed in a three electrode assembly. Saturated calomel electrode (SCE) was used as the reference electrode. Platinum electrode having 1cm<sup>2</sup> area was taken as counter electrode. Metal specimens with an exposed area of 1cm<sup>2</sup> were used as the working electrode. The EIS experiments were carried out on an Ivium compactstat-e electrochemical system. 100 ml of 0.5M H<sub>2</sub>SO<sub>4</sub> with A9Y5GPA and A9Y5GPA + 2ml KI (no stirring) were taken as the electrolyte and the working area of the metal specimens were exposed to the electrolyte for 1 h prior to the measurement. EIS measurements were performed at constant potential (OCP) in the frequency range from 1 KHz to 100 mHz with amplitude of 10 mV as excitation signal. The percentage of inhibitions from

impedance measurements were calculated using charge transfer resistance values by the following expression<sup>11</sup>:

$$EIS \% = \frac{R_{ct} - R'_{ct}}{R_{ct}} \times 100 \quad \dots(3)$$

where R<sub>ct</sub> and R'<sub>ct</sub> are the charge transfer resistances of working electrode with and without inhibitor respectively.

Polarization plots were obtained in the electrode potential range from -100 to +100 mV Vs equilibrium potential (E<sub>corr</sub>) at a scan rate of 1mV/sec. Tafel polarization analysis were done by extrapolating anodic and cathodic curves to obtain corrosion current densities (I<sub>corr</sub>). The percentage of inhibition efficiency ( $\eta_{pol}\%$ ) was evaluated from the measured I<sub>corr</sub> values using the relation :

$$\eta_{pol} \% = \frac{I_{corr} - I'_{corr}}{I_{corr}} \times 100 \quad \dots(4)$$

where I<sub>corr</sub> and I'<sub>corr</sub> are the corrosion current densities of the exposed area of the working electrode in the absence and presence of inhibitor. Surface analyses were performed using scanning electron microscope (model Hitachi SU6600).

## RESULTS AND DISCUSSION

### Weight Loss Measurements

The calculated values of inhibition efficiency ( $\eta_w\%$ ) and surface coverage ( $\theta$ ) at 30°C from the losses of weight of CS after immersing in solutions of 0.5 M H<sub>2</sub>SO<sub>4</sub> containing different concentrations of the A9Y5GPA are given in table 1.

From table 1 it is clear that the inhibition efficiency increases with increasing the concentration of the compound. Various concentrations of A9Y5GPA alone show very low inhibition values. This behaviour indicates that the A9Y5GPA can act as a moderate inhibitor for CS corrosion in 0.5M H<sub>2</sub>SO<sub>4</sub> solution. However the A95GPA + KI system shows high inhibition values. The inhibitive action of the used compound is attributed to the adsorption of molecules on CS surface, forming a barrier between the metal surface and the corrosive environment.

**Table 1: Calculated values of inhibition efficiency ( $\eta_w$ %) for CS corrosion in 0.5M H<sub>2</sub>SO<sub>4</sub>**

Systems/concentrations	Corrosion Rate (mm/y)	Inhibition efficiency ( $\eta_w$ %)	$\omega$
Blank	24.01	-	-
Blank + 0.2mM KI	19.40	19.16	0.19
0.2 mM A9Y5GPA	20.37	15.14	0.15
0.4 mM A9Y5GPA	19.36	19.36	0.19
0.6 mM A9Y5GPA	18.13	24.48	0.24
0.8 mM A9Y5GPA	16.93	29.50	0.29
1.0 mM A9Y5GPA	15.21	36.65	0.36
0.2 mM A9Y5GPA + 0.2mM KI	7.70	67.94	0.68
0.4 mM A9Y5GPA + 0.2mM KI	6.61	72.45	0.72
0.6 mM A9Y5GPA + 0.2mM KI	4.87	79.71	0.79
0.8 mM A9Y5GPA + 0.2mM KI	4.16	82.65	0.83
1.0 mM A9Y5GPA + 0.2mM KI	3.52	85.34	0.85

**Table 2: Synergism parameter ( $S_\theta$ ) for different concentrations of A9Y5GPA in combination with 0.2mM KI**

Concentration	Synergism Parameter, $S_\theta$
0.2 mM	2.24
0.4 mM	2.48
0.6 mM	3.18
0.8 mM	3.49
1.0 mM	3.71

**Table 3: Electrochemical impedance parameters of CS specimens in 0.5M H<sub>2</sub>SO<sub>4</sub> at 30°C in the absence and presence of A9Y5GPA (3a) and A9Y5GPA + 0.2 mM KI (3b)**

C (mM)	$R_{ct}$ ( $\Omega\text{cm}^2$ )	$C_{dl}$ ( $\mu\text{F cm}^{-2}$ )	$\eta_{EIS}\%$
3a			
0	8.9	135	-
0.2	11.90	123.1	25.21
0.4	15.78	104.3	43.60
0.6	23.20	91.4	61.64
0.8	29.94	83.8	70.27
3b			
0.2+KI	30.32	114.3	70.65
0.4+KI	47.87	100.7	81.41
0.6+KI	61.01	78.7	85.41
0.8+KI	147.80	75.7	93.98
1.0+KI	274.50	73.1	96.76

### Synergistic Effect

From table 1 it is also evident that  $\eta_w$  % for KI in combination with A9Y5GPA is higher than the sum of  $\eta_w$  % for single KI and single A9Y5GPA in all investigations, which is synergism in nature. Aramaki and Hackerman<sup>12</sup> calculated the synergism parameter  $S_\theta$  using the following equation:

$$S_\theta = \frac{1 - \theta_1 + 2}{1 - \theta_1 + 2} \quad \dots(5)$$

where  $1+2 = (1+2) - 12$ ;  $\theta_1$  = surface coverage by anion;  $\theta_2$  = surface coverage by cation;  $\theta'_{1+2}$  = measured surface coverage by both anion and cation.  $S_\theta$  approaches unity when there are no interactions between the inhibitor compounds, while  $S_\theta > 1$  points to a synergistic effect; in the case of  $S_\theta < 1$ , the antagonistic interaction prevails. The values of the synergism parameter for the various concentrations of A9Y5GPA studied from the gravimetric analysis are presented in table 2.

All values shown in this table are greater than unity. This is an indication for the enhanced inhibition efficiency obtained by the addition of iodide ions to A9Y5GPA is synergistic in nature<sup>13</sup>.

### Adsorption Studies

The best description of the adsorption behavior of A9Y5GPA and A9Y5GPA + KI on CS specimens in 0.5M H<sub>2</sub>SO<sub>4</sub> was Freundlich and Langmuir adsorption isotherms respectively. These

models are expressed as<sup>14</sup>

Freundlich adsorption isotherm

$$\theta = K_{ads} C \quad \dots(6)$$

Langmuir adsorption isotherm

$$\frac{\theta}{C} = \frac{1}{K_{ads}} + \theta \quad \dots(7)$$

where C is the concentration of the inhibitor,  $\theta$  is the fractional surface coverage and  $K_{ads}$  is the adsorption equilibrium constant. Figs. 2 and 3 represent the adsorption plots of A9Y5GPA and A9Y5GPA + KI obtained by the weight loss measurements of CS steel specimens in 0.5M  $H_2SO_4$  at 30°C for 24 h respectively.

The adsorption equilibrium constant  $K_{ads}$  is related to the standard free energy of adsorption  $\Delta G_{ads}^0$ , by

$$\Delta G_{ads}^0 = -RT \ln(55.5 K_{ads}) \quad \dots(8)$$

Where 55.5 is the molar concentration of water, R is the universal gas constant and T is the temperature in Kelvin<sup>15</sup>. In the present study, A9Y5GPA and A9Y5GPA + KI molecules showed  $\Delta G_{ads}^0$  -24.2 KJ and -27.5 KJ respectively, suggesting that the adsorption of inhibitor involves both electrostatic and chemical interactions.

### Electrochemical Investigations

Figs.4 and 5 represent the Nyquist plots of CS specimens in 0.5M  $H_2SO_4$  in the presence of various concentrations of A9Y5GPA and A9Y5GPA + KI respectively. It is evident from the plots that the impedance response of metal specimens has marked difference in the presence and absence of the KI with A9Y5GPA.

Impedance behaviour can be well explained by pure electric models that could verify and enable to calculate numerical values corresponding to the physical and chemical properties of electrochemical system under examination<sup>16</sup>. The simple equivalent circuit that fit to many electrochemical systems composed of a double layer capacitance ( $C_{dl}$ ), solution resistance ( $R_s$ ) and charge transfer resistance ( $R_{ct}$ )<sup>17, 18</sup>. The impedance parameters are tabulated in the table 3 (3a and 3b).

The capacitance values  $C_{dl}$  decreases with A9Y5GPA concentration and this decrease in  $C_{dl}$  is enhanced upon addition of I<sup>-</sup> ions to the corrosive environment. These results suggest that the A9Y5GPA molecules function by adsorption at the metal/solution interface<sup>19</sup> and this adsorption is reinforced by I<sup>-</sup> ions. The  $\tau_{EIS\%}$  data reveal that the corrosion inhibition capacity of A9Y5GPA is markedly enhanced by the addition of KI.

**Table 4: Potentiodynamic polarization parameters of CS specimens in 0.5M  $H_2SO_4$  at 30°C**

C(mM)	$E_{corr}$ (mV/SCE)	$I_{corr}$ (mA/cm <sup>2</sup> )	$b_a$ (mV/dec)	$-b_c$ (mV/dec)	$\eta_{pol\%}$
A9Y5GPA Alone					
0	-467	1.170	0.082	0.124	-
0.2	-475	0.831	0.072	0.126	28.97
0.4	-494	0.7102	0.071	0.102	39.30
0.6	-541	0.6304	0.080	0.119	46.12
0.8	-461	0.4316	0.063	0.123	63.11
1.0	-488	0.2656	0.065	0.105	77.30
A9Y5GPA + 2ml KI					
0	-467	1.170	0.082	0.124	-
0.2	-472	0.2297	0.072	0.100	80.37
0.4	-475	0.1495	0.058	0.101	87.22
0.6	-482	0.1261	0.099	0.100	89.22
0.8	-475	0.0545	0.037	0.097	95.34
1.0	-466	0.0335	0.053	0.089	97.14

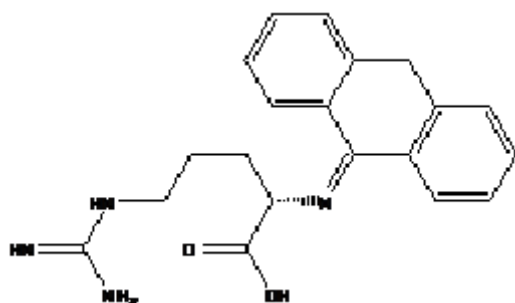


Fig. 1: Molecular Structure of A9Y5GPA

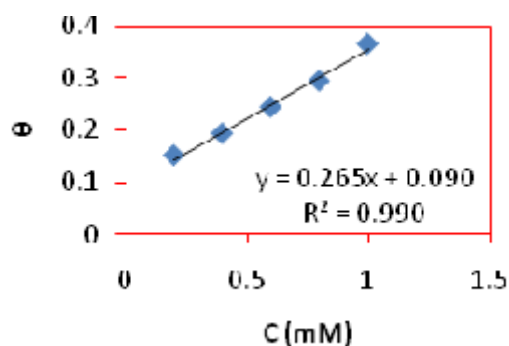


Fig. 2: Freundlich adsorption isotherm for adsorption of A9Y5GPA on CS surface

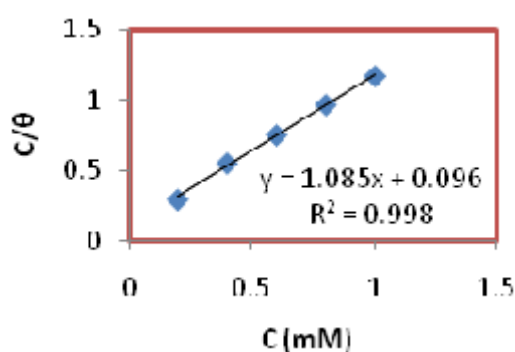


Fig. 3: Langmuir adsorption isotherm for adsorption of A9Y5GPA + KI on CS surface

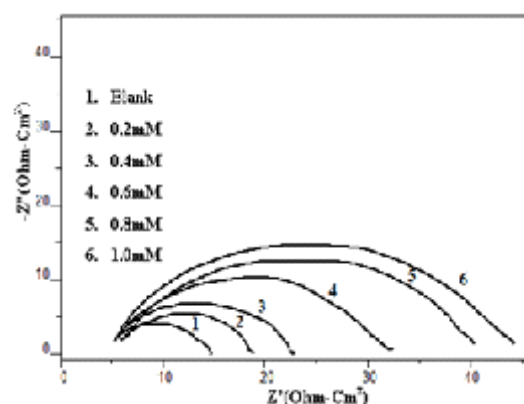


Fig. 4: Nyquist plots for CS specimens in A9Y5GPA solutions

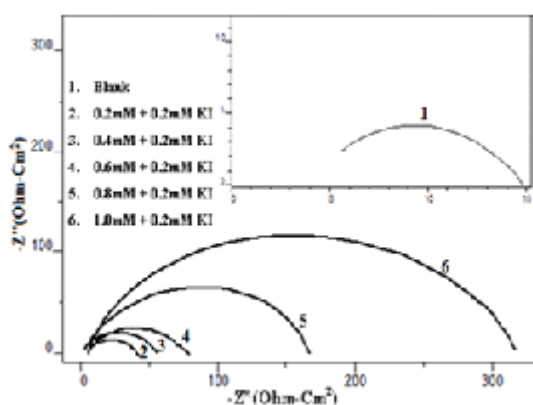


Fig. 5: Nyquist plots for CS specimens in A9Y5G PA + KI solutions

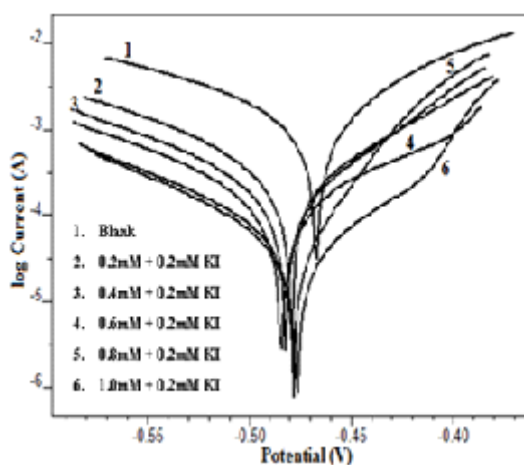


Fig. 6: Tafel plots

Potentiodynamic polarization curves for A9Y5GPA in 0.5M H<sub>2</sub>SO<sub>4</sub> at 30 °C for CS specimens in the presence of various concentrations of A9Y5GPA and A9Y5GPA + KI are shown in Fig.6 and Fig.7 respectively.

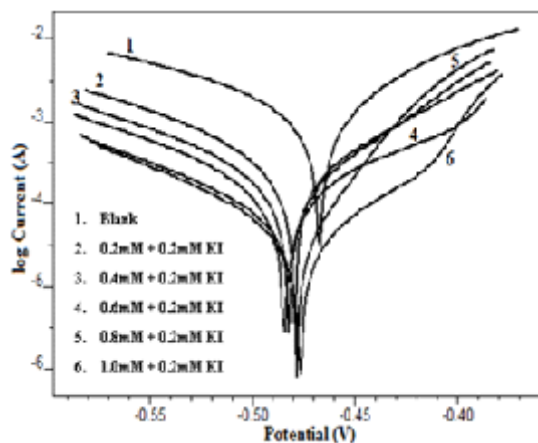


Fig. 7: Tafel plots (Synergistic Effect)

Polarization parameters like corrosion current densities ( $i_{corr}$ ), corrosion potential ( $E_{corr}$ ), cathodic Tafel slope ( $b_c$ ), anodic Tafel slope ( $b_a$ ), and inhibition efficiency ( $\eta_{pol\%}$ ) for CS specimens are listed in table 4. The data show that, addition of the A9Y5GPA to acid media affected both the cathodic and anodic parts of the curves. Addition of I<sup>-</sup> ions to A9Y5GPA - H<sub>2</sub>SO<sub>4</sub> systems results in marked decrease in the corrosion current density ( $i_{corr}$ ). The maximum shift of  $E_{corr}$  is 74mV, suggesting that A9Y5GPA acts as a mixed type inhibitor for CS specimens in 0.5M H<sub>2</sub>SO<sub>4</sub>. From the values it is clear that the inhibition efficiency of A9Y5GPA alone is increased in presence of KI. These results also confirm the existence of strong synergism between A9Y5GPA and KI in the corrosion inhibition of CS in these solutions.

#### SEM Studies

The surface morphology of carbon steel surface was evaluated by scanning electron microscopy (SEM). Figures 8 (A, B, C and D) show

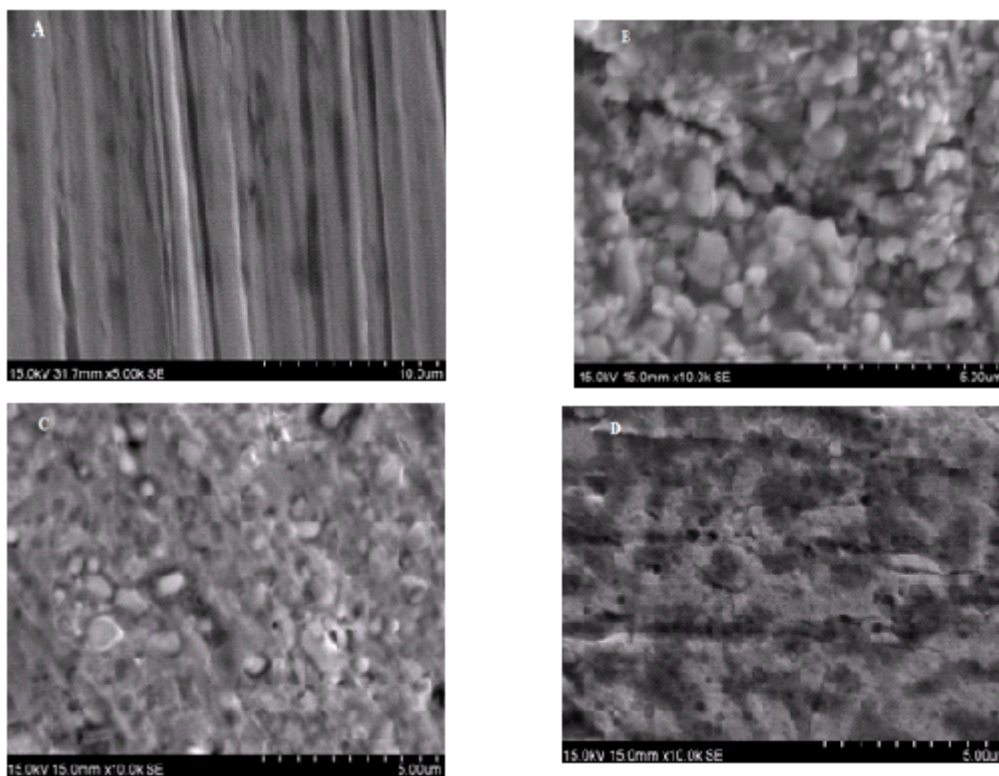


Fig.8 Scanning Electron Micrographs of carbon steel samples: A) Polished fresh specimens B) Immersed in 0.5M H<sub>2</sub>SO<sub>4</sub> solution C) Immersed in 0.5M H<sub>2</sub>SO<sub>4</sub> solution with 1mM A9Y5GPA C) Immersed in 0.5M H<sub>2</sub>SO<sub>4</sub> solution with 1mM A9Y5GPA+ 1ml KI

the scanning electron micrographs of the bare carbon steel surface, CS specimens in  $H_2SO_4$ , with A9Y5GPA and with A9Y5GPA+ KI in  $H_2SO_4$  medium for 24 h respectively. The morphology revealed that in the absence of A9Y5GPA, the surface is highly corroded. However in the presence of A9Y5GPA the rate of corrosion is suppressed and the SEM image D shows that inhibition action enhanced by forming a protective layer on the surface that prevents the attack of acid on the corroding metal CS.

#### Mechanism and Explanation for synergism

The synergistic inhibition brought about by the combination of A9Y5GPA and iodide ions for the corrosion of CS in 0.5 M  $H_2SO_4$  can be explained on the basis that halide ions have a greater tendency to be adsorbed on the surface in attraction with organic cations.

The protonated Schiff base (A9Y5GPA<sup>+</sup>) is adsorbed by coulombic attraction at the steel surface, where iodide ions are already adsorbed by chemisorptions. Greater surface coverage from the stabilization of adsorbed iodide ions by means of electrostatic interaction with A9Y5GPA<sup>+</sup> facilitates corrosion inhibition synergism.

#### CONCLUSIONS

1. Inhibition efficiency increases with increase in concentration of inhibitor.
2. The addition of iodide ions to A9Y5GPA enhanced the inhibition efficiency due to synergistic effect.
3. The adsorption of A9Y5GPA alone and in combination with iodide ions obeys Freundlich and Langmuir adsorption isotherms respectively.
4. The thermodynamic parameters calculated from the adsorption isotherms showed that both physisorption and chemisorptions are involved in the inhibition process.

#### REFERENCES

1. James, O.; Oforka, N. C.; Abiola, O.K. *Int. J. Electrochem. Sci.* **2007**, *2*, 278-284
2. Sethi, T. A.; Chaturvedi, R. K.; Upadhyay; Marthur, S. P. *J. Chil. Chem. Soci.* **2007**, *52*, 1206-1213
3. Srivastva, K. P.; Kumar, A.; Singh, R. *J. Chem. Pharm. Res.* **2010**, *2*, 68-77
4. Ade, S. B.; Deshpande, M. N.; Kolhatkar, D. G. *J. Chem. Pharm. Res.* **2012**, *4*, 1033-1035
5. Vinod, P. R.; Joby, T.K.; Shaju, K.S.; Aby, P. *Res. Chem. Intermed.* **2013**, DOI 10.1007/s11164-013-1122-3
6. Aby, P.; Joby, T.K.; Vinod, P. R.; Shaju, K.S. *Orient. J. Chem.* **2012**, *28*, 1501-1507
7. Shaju, K.S.; Joby, T.K.; Vinod, P.R.; Aby, P. Hindawi Publishing Corporation, *ISRN Corrosion.* **2012**, <http://dx.doi.org/10.5402/2012/4258>
8. Shaju, K. S.; Joby, T.K.; Vinod, P. R.; Aby, P. Hindawi Publishing Corporation, *ISRN Electrochemistry.* **2013**, <http://dx.doi.org/10.1155/2013/820548>
9. Deng, S.; Li, X.; Fu, H. *Corros. Sci.* **2011**, *53*, 3704-3711
10. Emregul, K.C.; Atakol, O. *Mater. Chem. Phys.* **2004**, *83*, 373-379
11. Ashassi-Sorkhabi, H.; Shaabani, B.; Seifzadeh, D. *Electrochim. Acta.* **2005**, *50*, 3446-3452
12. Aramaki, K.; Hackerman, M. *J. Electrochem. Soc.* **1969**, *116*, 568-574
13. Caliskan, N.; Bilgic, S. *Appl. Surf. Sci.* **2000**, *153*, 128-133
14. Bouklah, M.; Hammouti, B.; Lagrenée, M.; Bentiss, F. *Corros. Sci.* **2006**, *48*, 2831-2842
15. Cano, E.; Polo, J.L.; Iglesia, A.L.A.; Bastidas, J.M. *Adsorption.* **2004**, *10*, 219-225
16. Priya, A.R.S.; Muralidharam, V.S.; Subramannia, A. *Corrosion.* **2008**, *64*, 541-552
17. Azhar, M.E.; Mernari, B.; Traisnel, M.; Bentiss, F.; Lagrenée, M. *Corros. Sci.* **2001**, *43*, 2229-2238
18. Yurt, A.; Balaban, A.; Kandemir, S.U.; Bereket, G.; Erk, B. *Mater. Chem. Phys.* **2004**, *85*, 420-426
19. McCafferty, M.; Hackerman, N. *J. Electrochem. Soc.* **1972**, *119*, 146-154